Supporting Information

An intelligent and portable power storage device enable visualize energy status

Lei Liu, Qianqian Zhang, Kai Du, Zhibing He, Tao Wang, Yong Yi, Mengying Wang, Xiaolan Zhong, Guobo Dong and Xungang Diao**

Content of Supporting Information

1. Top-view SEM images of single layers in the EPSD

In the EPSD, each layer composed of nanoparticles had a flat and uniform surface (Figure S1).

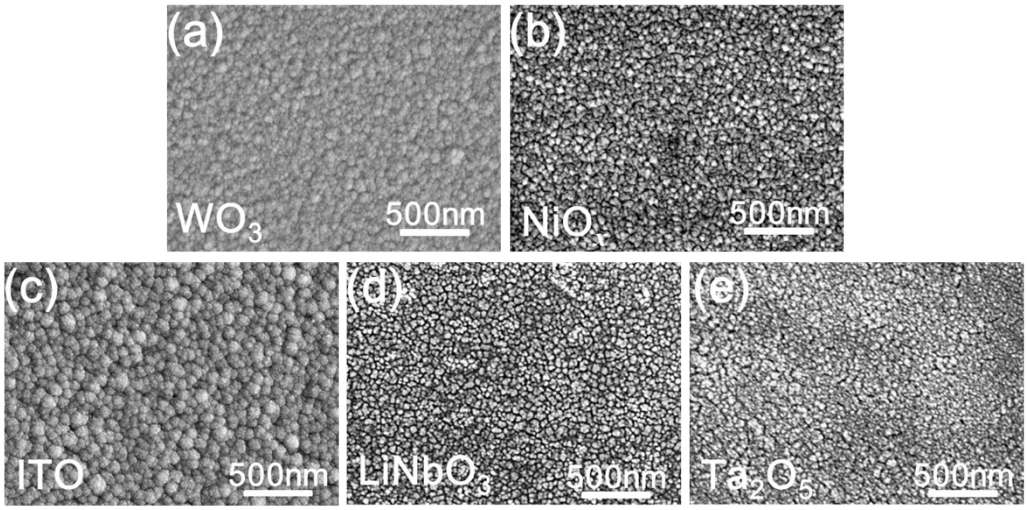

Figure S1. Top-view SEM images of WO_3 layer (a), NiO_x layer (b), ITO layer (c), $LiNbO_3$ layer (d) and Ta_2O_5 layer (e) of the EPSD.

2. Transmittance spectra of the WO_3 and NiO_x at colored and bleached states

The transmittance spectra of the WO_3 and NiO_x films between the colored and bleached states were shown in Figure S2. The digital optical images of as-deposited WO_3 and NiO_x in colored state and bleached state are shown in the inset of Figure S3. It can be seen that NiO_x film presents deep brown when the applied potential at 1.5 V, while the WO_3 film shows dark blue as the applied potential at -1 V and the character on the paper hardly can be seen.

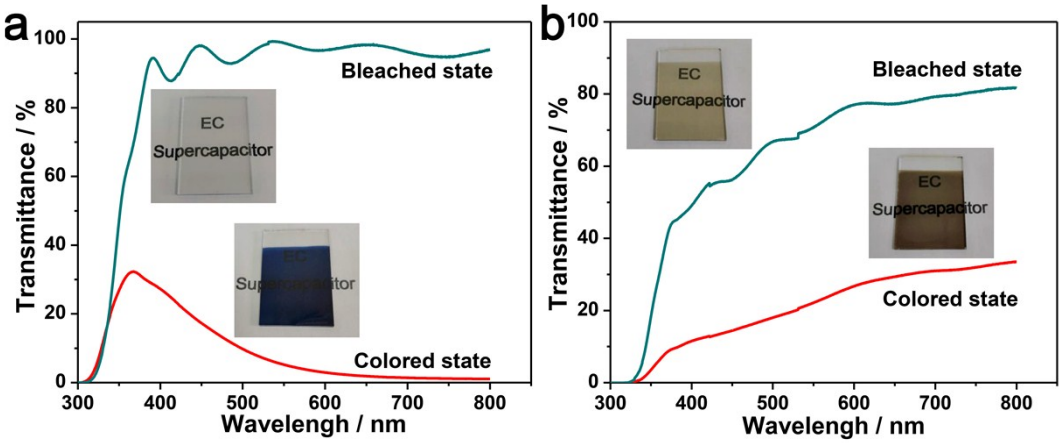

Figure S2. Transmittance spectra of the WO_3 and NiO_x films in bleached and colored states in the wavelength range of 300-800nm. Insets: The digital paragraphs of WO_3 and NiO_x films at bleached and colored states.

3. XRD patterns about single layer of EPSD

As shown in Figure S3a, no resolved diffraction peaks were detected from the XRD pattern of the WO_3 film at original, colored and bleached states, indicating an amorphous phase.[1] The XRD pattern of the NiO_x is in accordance with the standard face-centered cubic NiO (JCPDS card No. 47-1049), and the characteristic peaks has no shift in response to charging state (Figure S3b). Therefore, no phase transition occurred in WO_3 and NiO_x during charge/discharge process of the EPSD.[2] The XRD curves of other layers were shown in the Figure S3c.

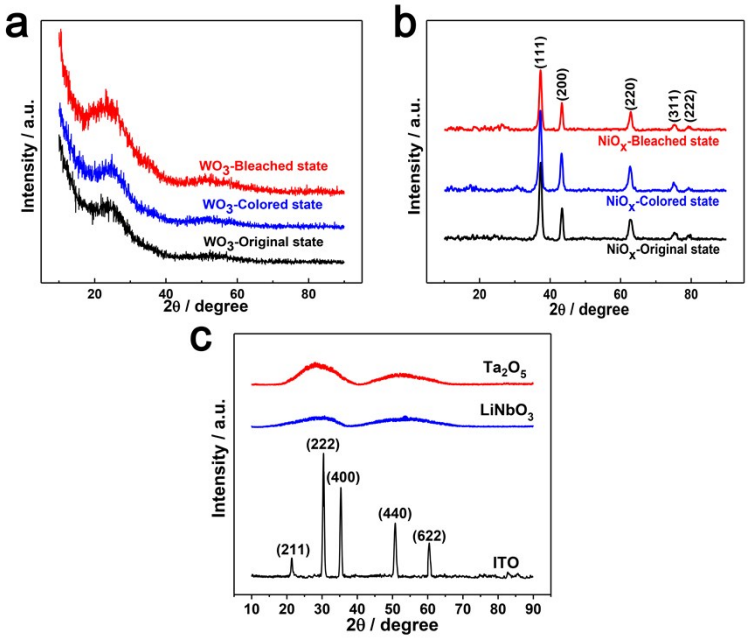

Figure S3. XRD patterns about single layer of EPSD.

4. XPS patterns about single layer of EPSD

The XPS spectra of In3d and Sn3d doublet peaks for ITO film are shown in Fig. S4a, b, respectively. These show the evidence of only one binding state for In and Sn since there is no sign of broadening or splitting of the peaks. The XPS peaks of Li1s and Nb3d obtained for $LiNbO_3$ films are plotted in Fig. S4c, d. Core line spectrum for Li 1s is observed at 55.2 eV near Nb4s lines. The peaks at 207.2 and 209.8 eV correspond to electronic state of $Nb3d_{5/2}$ and $Nb3d_{3/2}$ respectively. The XPS peaks of Ta 4f and O 1s spectra obtained for Ta_2O_5 films are plotted in Fig. S4e, f.

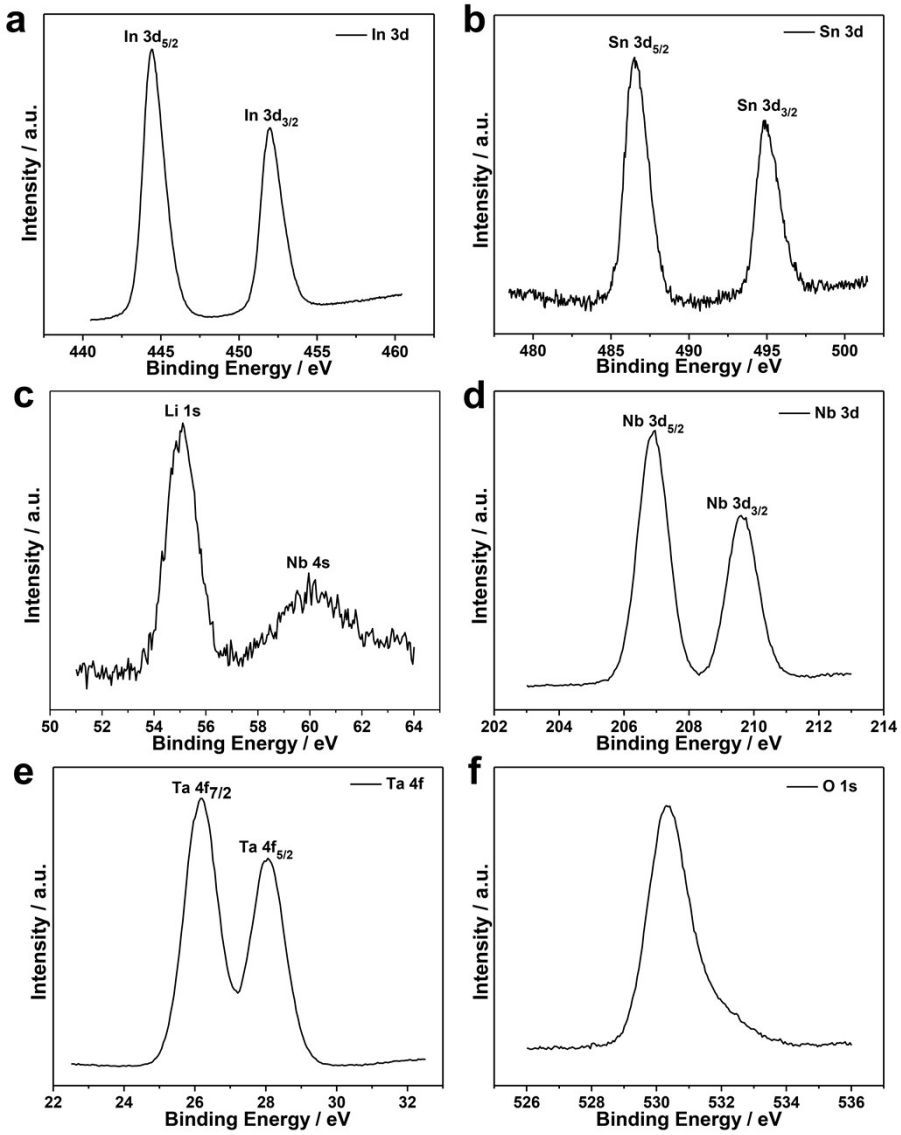

Figure S4. XPS patterns about single layer of EPSD.

5. The electrochemical behavior and cycling stability of WO_3 and NiO_x single electrodes

The electrochemical studies for the WO_3 and NiO_x single electrodes were conducted in a three-electrode configuration using 1M PC-$LiClO_4$ electrolyte. The volume capacitances of WO_3 and NiO_x single electrodes are calculated based on the CV curves at different scan rates and shown in Figure S5a. The cycle performances of the electrode for 5000 consecutive CV curves at a scan rate of 50 mv s^{-1} are shown in Figure S5b. The capacitance retentions of WO_3 and NiO_x single electrodes are 98.5% and 96.8%, respectively. Figure S5c and S5d show the colored and bleached transmittance at 550 nm of single electrode, which varies as a function of cycle number. The WO_3 film sustained a transmittance modulation of about 95.3% of the initial value after 5000 cycles. The NiO_x film sustained a transmittance modulation of about 94.5% of the initial value even subjected to 5000 cycles.

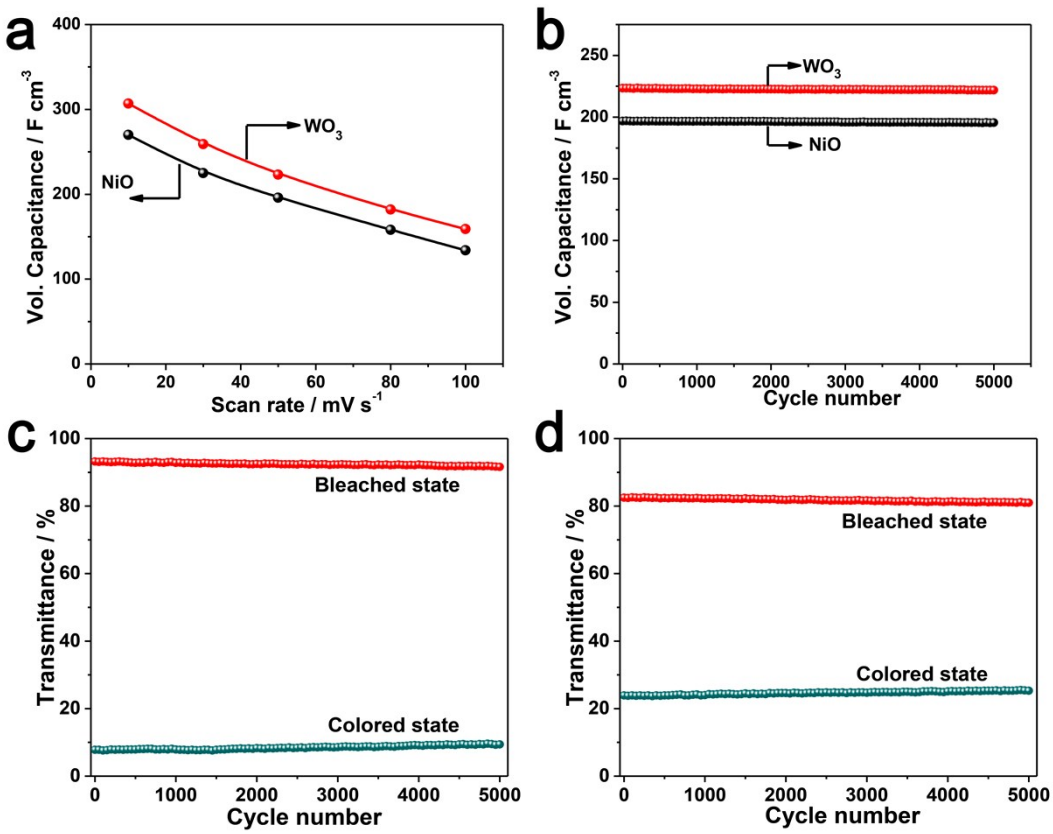

Figure S5. (a) Volume capacitance calculated from the CV curves as a function of scan rate. (b-d) Cyclic stability of WO_3 and NiO_x single electrodes tested for 5000 cycles.

6. CV curves of EPSD at extended potential window

Figure S6a presents the CV curves in -1.5-2.3 V and -1.5-2.5 V potential window at 50 mV s^{-1} scan rate, in order to investigate the performance of the EPSD at extended potential window. Unfortunately, obvious leakage current was existed at the end of discharge process. Some defects may be formed in the ions electrolyte layer or the electrochromic layers or the interface among layers, mainly cause that electrons contributing to leakage current could be smoothly kinetically transferred through these layers under such widen external potential.[3] The cycle stability of the EPSD at widen voltage window was investigated, larger leakage current in the device that leads to a lower capacity after 1000 CV cycles.

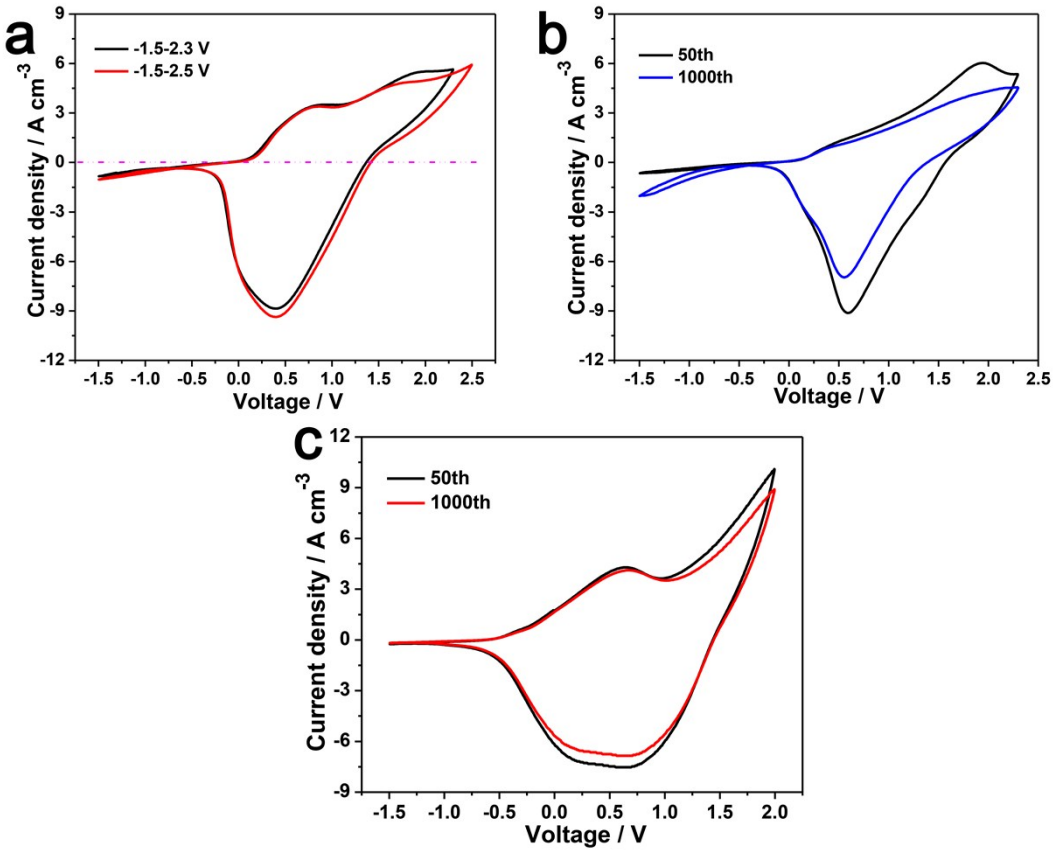

Figure S6. (a) The CV behaviors of the EPSD in a voltage window of -1.5-2.3 V and -1.5-2.5 V at a scan rate of 50 mV s^{-1}, (b) CV cyclic stability of the EPSD recorded from -1.5 to 2.3 V at a scan rate of 50 mV s^{-1}, (c) CV cyclic stability of the EPSD recorded from -1.5 to 2.0 V at a scan rate of 50 mV s^{-1}.

7. CV curves of the EPSD in different potential windows at various scan rates

Figure S7 shows the CV curves of EPSD in different potential windows at various scan rates. Clearly, the CV curves retain similar shape even when the potential window at -1.5-2.0 V, suggesting good rate performance and high reversibility behavior of the EPSD in wide voltage windows.[4]

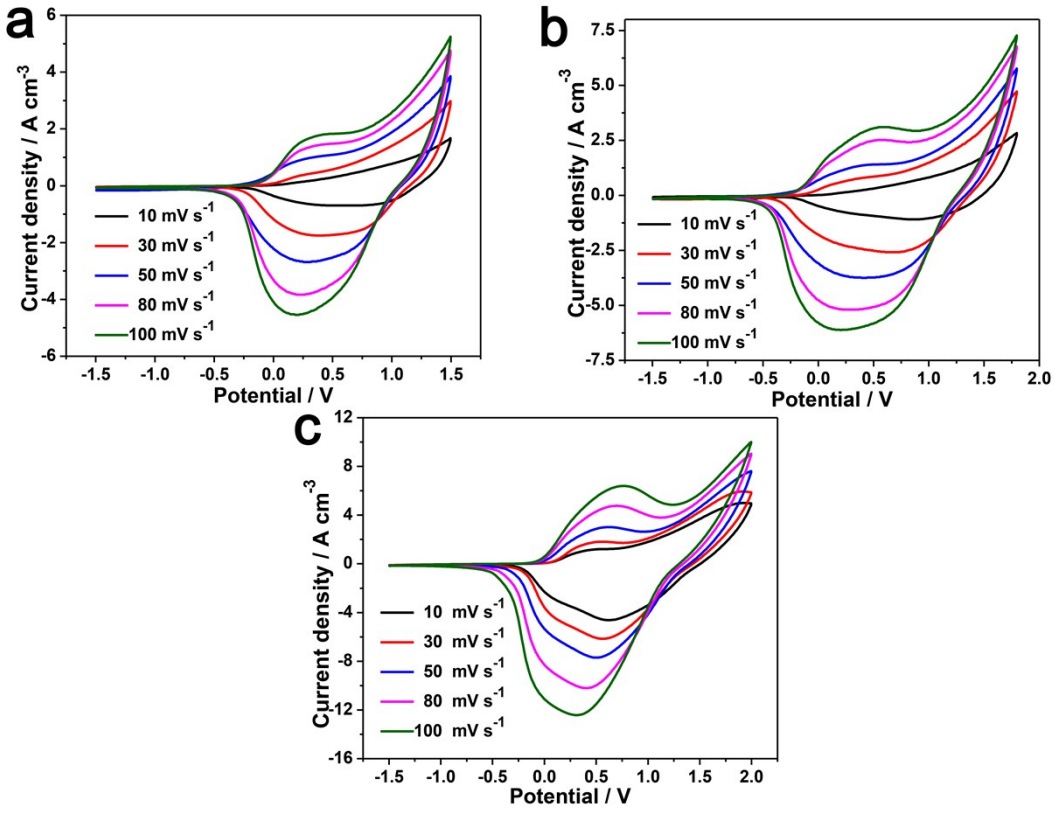

Figure S7. CV curves of the EPSD in different voltage windows of -1.5-1.5 V (a), -1.5-1.8 V (b) and -1.5-2.0 V (c) at different scan rates.

8. EIS spectra of the EPSD

The electrochemical performance of the EPSD was further evaluated using electrochemical impedance spectroscopy (EIS) with frequency ranging from 10 mHz to 100 kHz. EIS measurements of the EPSD were conducted at the colored state. The Nyquist plot exhibits a semicircle at the high-frequency range and shows a sloping line at the low-frequency region. As illustrated in the equivalent circuit (inset, Figure S8), these resistor and capacitor elements in the equivalent circuit are associated with specific parts of the Nyquist plot. R_s is the internal resistance, R_{ct} is the charge-transfer resistance, C_{dl} is the double-layer capacitance, C_l is the lowfrequency mass capacitance, and R_{leak} is the low-frequency leakage resistance. EIS spectrum of the EPSD shows a lower charge transfer resistance, implying fast faradaic reactions at both anode and cathode (Figure. S8).

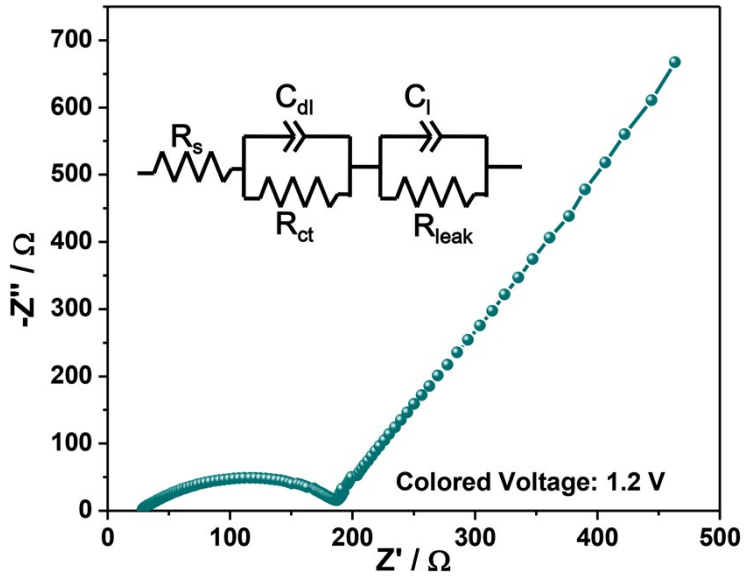

Figure S8. EIS spectra of the EPSD

9. Charge/discharge curves of the EPSD in different voltage windows at different current densities

For further investigation of the rate performance of the EPSD in different potential windows, charge/discharge measurements were carried out at various current densities from 1 to 16 A cm^{-3} (Figure S9).

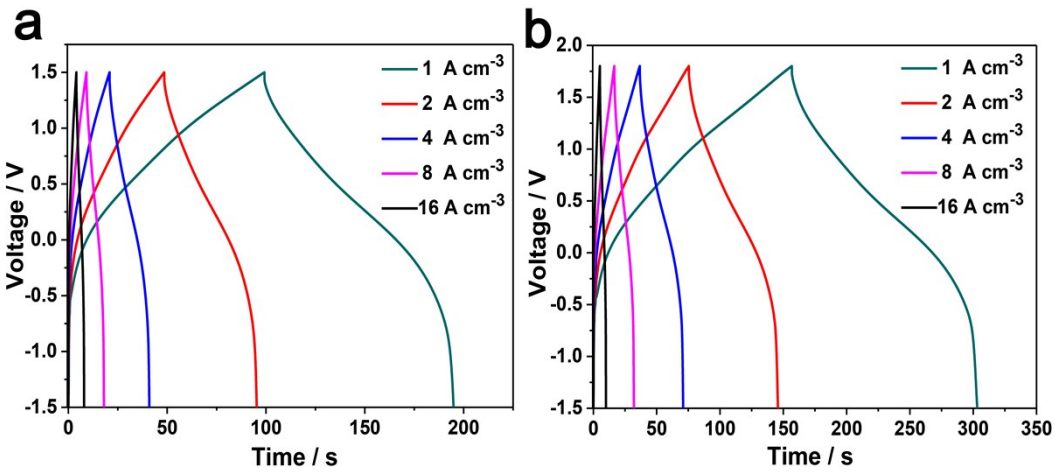

Figure S9. Charge/discharge curves of the EPSD in different voltage windows of -1.5-1.5 V (a) and -1.5-1.8 V (b) at different current densities.

10. Charge/discharge curves of the EPSD at higher current densities

The color of smart EPSD changes from transparent (bleached state) to dark blue (colored state) during charging process, while the color fades away in the reverse process. The device can still present the level of stored energy by a rapid and reversible color variation even at a high current density of 4 A cm^{-3} (Figure S10). Therefore, the energy storage level can be visually monitored by the color change.

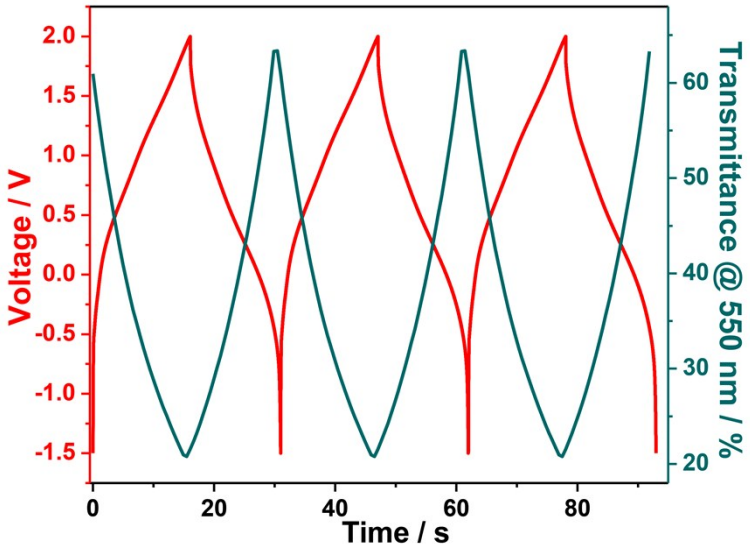

Figure S10. Galvanostatic charge/discharge profile at 4 A cm^{-3} in the voltage window of -1.5 to 2.0 V and corresponding *in situ* optical response measured at 550 nm for the EPSD.

11. Areal capacitance of the EPSD

The areal capacitance of the EPSD based on CV curves with various scan rates at different voltage windows was shown in Figure S11.

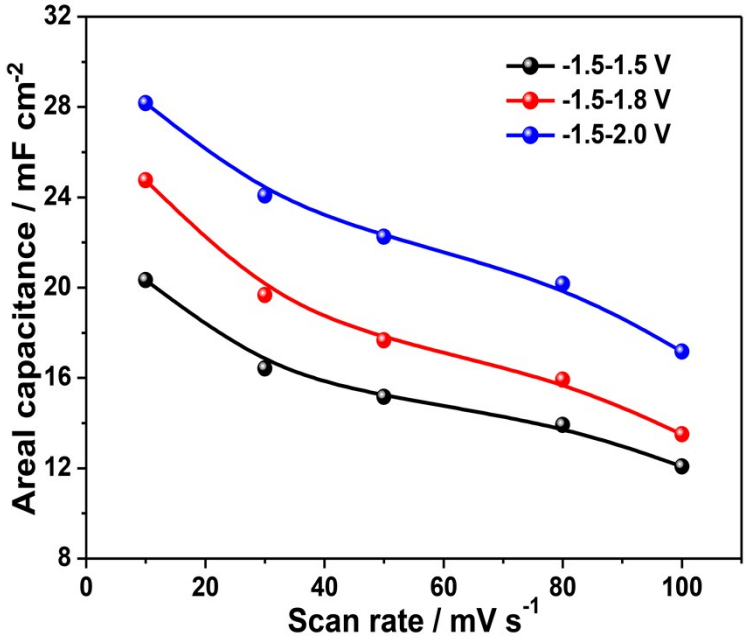

Figure S11. Areal capacitance of the EPSD

12. Long-term consecutive CV cyclic behavior of the EPSD

Cycle performance of the EPSD measured in the potential range of -1.5 to 2.0 V for 5000 cycles (Figure S12). Clearly, slight degradation of the EPSD was presented. On the one hand, some active Li^+ ions were trapped in electrochromic layers may be most likely the main factors contributing for charge capacity fade of the EPSD.[5] On the other hand, irreversible damage of physical and chemical structures such as mechanical cracks within layers and interfaces between layers in the EPSD also impedes the Li^+ ions transfer kinetics among layers.[6]

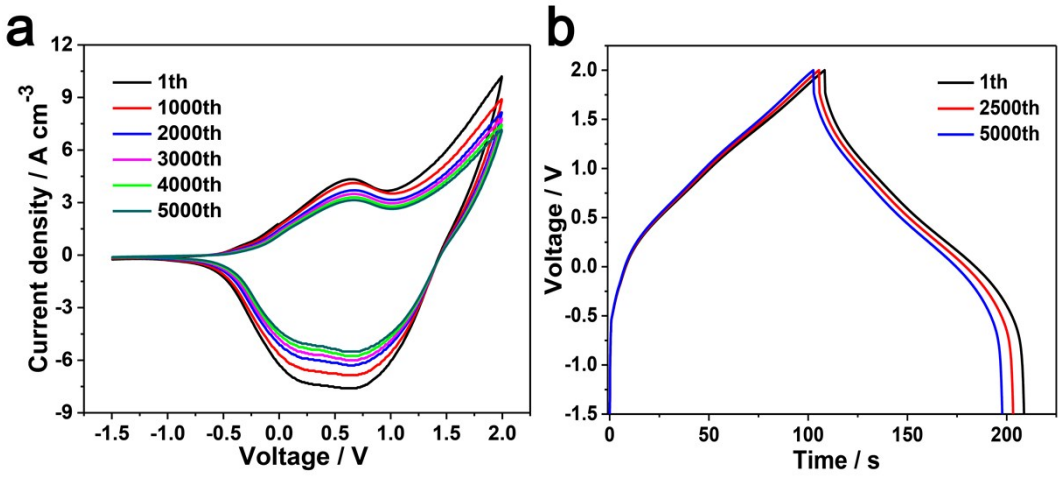

Figure S12. Long-term consecutive behaviors of the EPSD: (a) CV at 50 mV s^{-1} scan rate and GCD at 2 A cm^{-3} current density.

13. Optical memory effects and open-circuit potentials of the EPSD

The introduction of Ta_2O_5 separator layers effectively enhanced the memory effects of the open-circuit potential and optical property of the EPSD. As shown in Figure S13, the open-circuit potential and transmittance at 550nm could remain stable for a long while with the presence of Ta_2O_5 separators. The two Ta_2O_5 layers could provide sufficient energy barriers to prevent electrons transferring into the electrolyte.[7] This effectively reduced the leakage current of the EPSD. A lower leakage current suggests that a higher potential could effectively apply for the insertion of Li^+ ions into WO_3 or NiO_x layer, which would lead to a higher energy density.[8]

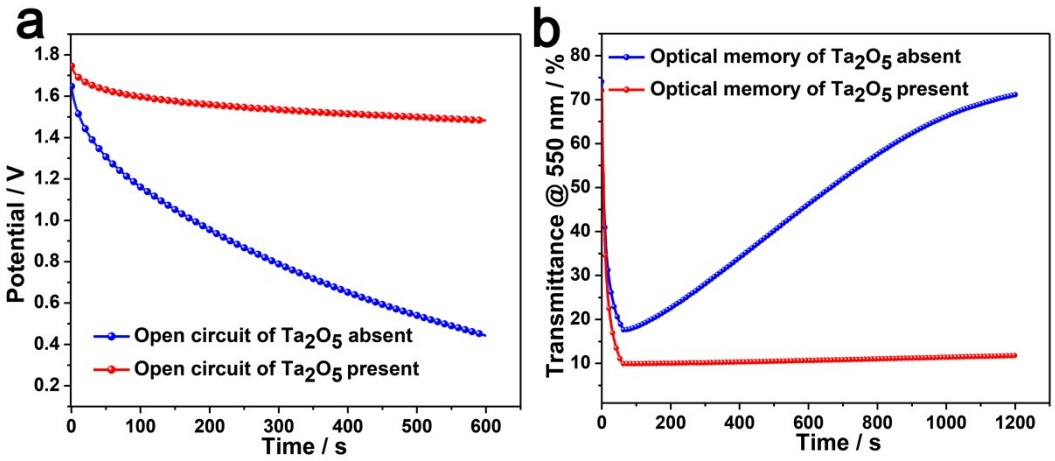

Figure S13. Open-circuit potentials (a) and optical memory effects (b) of the EPSD.

14. Optical images of the EPSD lighting a LED at different time durations

On the level of practical application, the prototype device was employed to power a 1.5 V red light-emitting-diode (LED) and successfully lightened it for over 25s.

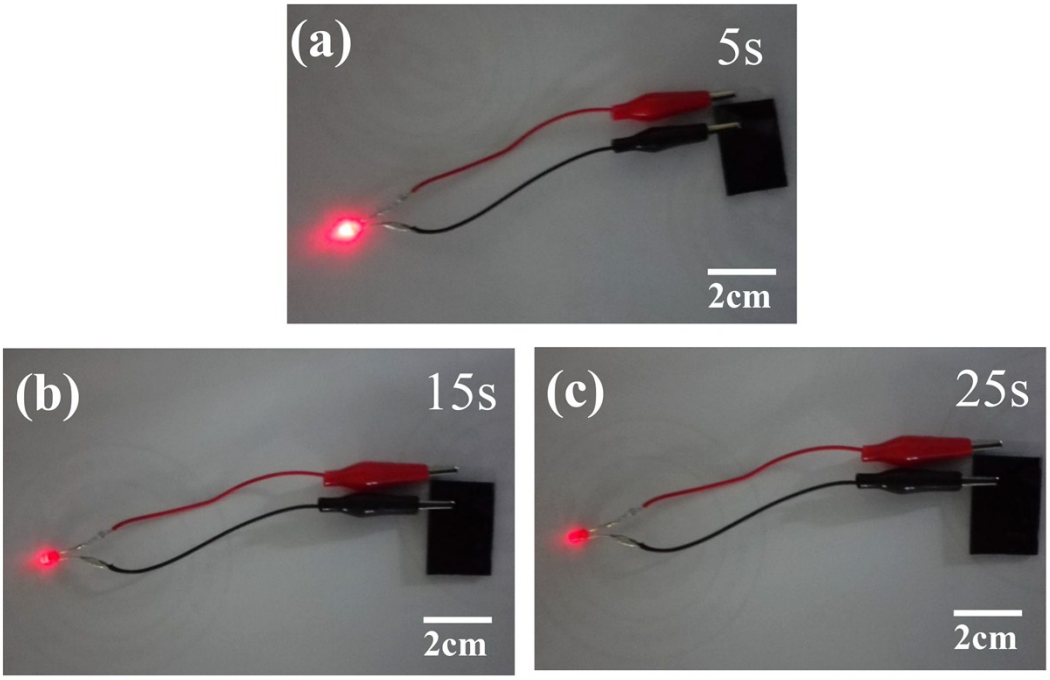

Figure S14. Optical images of the EPSD lighting a LED at different time durations.

15. SEM and XRD of the EPSD after cycling

From the SEM image we can see that the EPSD sustain its stable structure even the insertion Li^+ ions lead some volume expansion of the NiO_x and WO_3 materials (Figure S15a). The XRD results indicating that the phase of the components sustain stable even subjected to 5000 cycles (Figure S15 b, c).

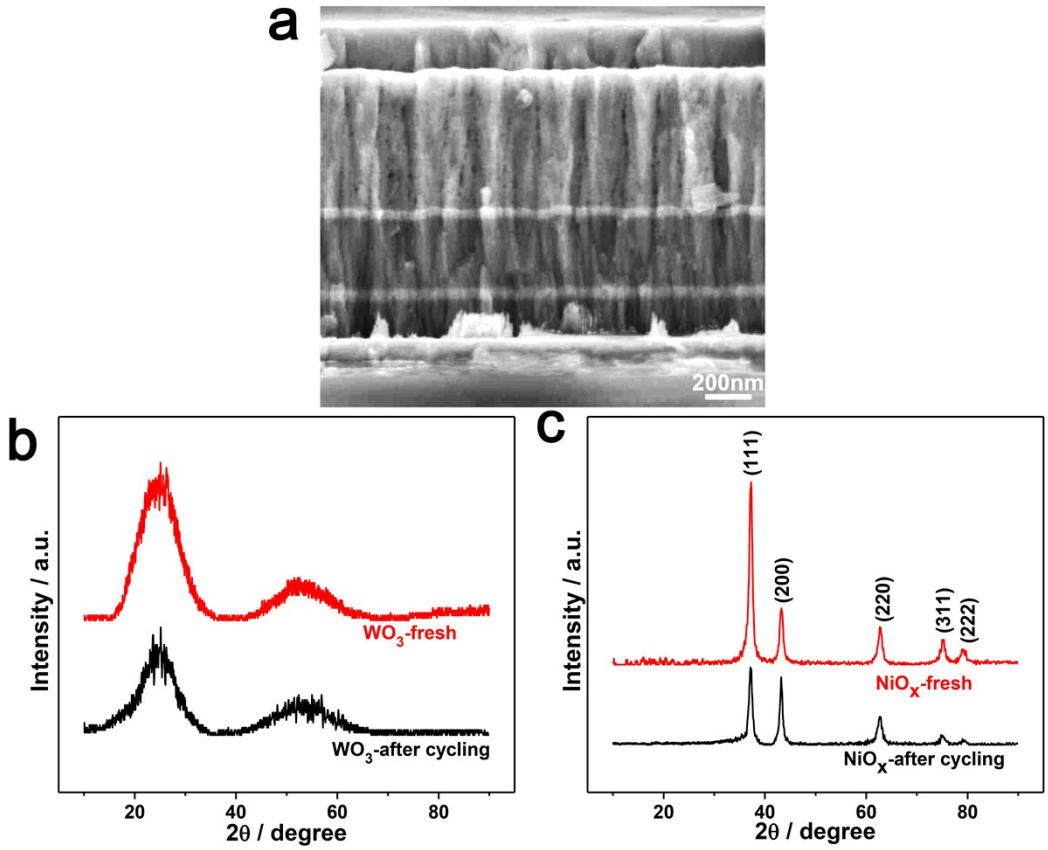

Figure S15. SEM and XRD of the EPSD after cycling

16. More details on the color changes of the EPSD

More details on the color changes of the EPSD during the capacitive process were provided separately in Figure S16. The test was performed in the voltage window from -1.5 V to 2.0 V with 50 mV s^{-1} scan rate.

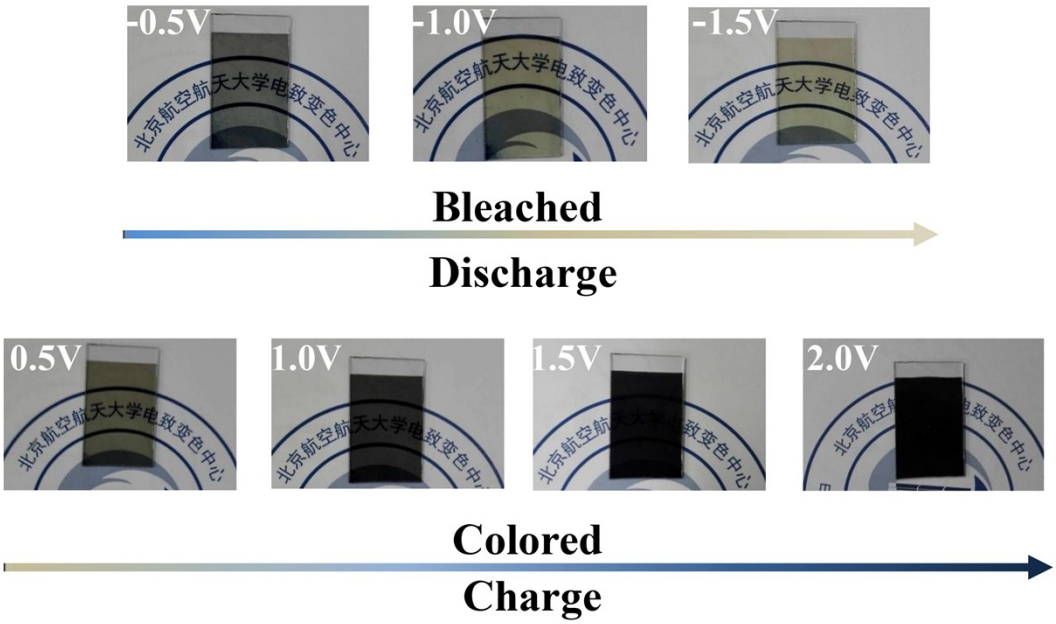

Figure S16. Digital photos of the EPSD showing different colors when at different voltages.

17. Detailed deposition parameters of all layers assembled into the EPSD

TableS1. Detailed deposition parameters of the layers in the EPSD

Layer	Target	Method	Working pressure/Pa	Gas flow/sccm		Power/W
				Ar	O_2	
NiO_x	Ni	DC MS[a]	1.5	270:35		230
Ta_2O_5	Ta	DC MS	0.3	140:60		275
$LiNbO_3$	$LiNbO_3$	RF MS[b]	0.6	190:10		300
WO_3	W	DC MS	2.0	300:100		350
ITO	ITO	DC MS	0.3	270:10		170

[a] Direct current magnetron sputtering

[b] Radio frequency magnetron sputtering

18. References

[1] G. Cai, M. Cui, V. Kumar, P. Darmawan, J. Wang, X. Wang, A. L. Eh, K. Qian, P. S. Lee, *Chem. Sci.* **2016**, *7*, 1373.

[2] Y. Wang, Y. Song, Y. Xia, *Chem. Soc. Rev.* **2016**, *45*, 5925.

[3] Q. Liu, G. Dong, Q. Chen, J. Guo, Y. Xiao, M. D. Ogletree, F. Reniers, X. Diao, *Sol. Energy Mater. Sol. Cells* **2018**,*174*, 545.

[4] G. Lee, D. Kim, J. Yun, Y. Ko, J. Cho, J. S. Ha, *Nanoscale* **2014**, *6*, 9655.

[5] R. T. Wen, C. G. Granqvist, G. A. Niklasson, *Nat. Mater.* **2015**, *14*, 996.

[6] D. Dong, W. Wang, A. Rougier, G. Dong, M. D. Rocha, L. Presmanes, K. Zrikem, G. Song, X. Diao, A. Barnabé, *Nanoscale*, DOI: 10.1039/c8nr02267d.

[7] A. Subrahmanyam, C. S. Kumar, K. M. Karuppasamy, *Sol. Energy Mater. Sol. Cells* **2007**, *91*, 62.

[8] K. Qi, X. Li, M. Sun, Q. Huang, J. Wei, Z. Xu, W. Wang, X. Bai, E. Wang, *Appl. Phys. Lett.* **2016**, *108*, 245.